Journal Pre-proofs

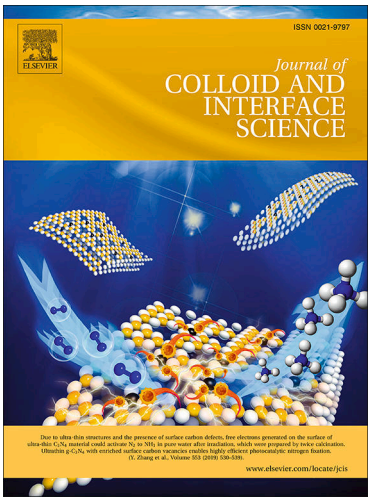

Regular Article

Household arsenic contaminated water treatment employing iron oxide/ bamboo biochar composite: an approach to technology transfer

Jacinta Alchouron, Chanaka Navarathna, Prashan M. Rodrigo, Annie Snyder, Hugo D. Chludil, Andrea S. Vega, Gianpiero Bosi, Felio Perez, Dinesh Mohan, Charles U. Pittman Jr., Todd E. Mlsna

PII: S0021-9797(20)31539-3
DOI: https://doi.org/10.1016/j.jcis.2020.11.036
Reference: YJCIS 27214

To appear in: *Journal of Colloid and Interface Science*

Received Date: 13 September 2020
Revised Date: 6 November 2020
Accepted Date: 8 November 2020

Please cite this article as: J. Alchouron, C. Navarathna, P.M. Rodrigo, A. Snyder, H.D. Chludil, A.S. Vega, G. Bosi, F. Perez, D. Mohan, C.U. Pittman Jr., T.E. Mlsna, Household arsenic contaminated water treatment employing iron oxide/bamboo biochar composite: an approach to technology transfer, *Journal of Colloid and Interface Science* (2020), doi: https://doi.org/10.1016/j.jcis.2020.11.036

Household arsenic contaminated water treatment employing iron oxide/bamboo biochar composite: an approach to technology transfer

Jacinta Alchouron [$,a]/ Chanaka Navarathna [$,b], Prashan M. Rodrigo [b], Annie Snyder [b], Hugo D. Chludil [c], Andrea S. Vega [a,d], Gianpiero Bosi [e], Felio Perez [f], Dinesh Mohan [g], Charles U. Pittman Jr. [b], Todd E. Mlsna [b,*]

[$] These authors have made an equal contribution

[a] Universidad de Buenos Aires, Facultad de Agronomía, Departamento de Recursos Naturales y Ambiente, Cátedra de Botánica General, Av. San Martín 4453, C1417DSE, Buenos Aires, Argentina

[b] Department of Chemistry, Mississippi State University, Mississippi State, MS 39762-9573, USA

[c] Universidad de Buenos Aires, Facultad de Agronomía, Departamento de Biología Aplicada y Alimentos, Cátedra de Química de Biomoléculas, Av. San Martín 4453, C1417DSE, Buenos Aires, Argentina

[d] Consejo Nacional de Investigaciones Científicas y Técnicas (CONICET), Buenos Aires, Argentina

[e] Universidad de Buenos Aires, Facultad de Arquitectura, Diseño y Urbanismo, Centro de Proyecto, Diseño, y Urbanismo (CEPRODIDE), Int. Güiraldes 2160, C1428EGA, Buenos Aires, Argentina

[f] Material Science Lab, Integrated Microscopy Center, University of Memphis, Memphis, TN 38152, USA

[g] School of Environmental Sciences, Jawaharlal Nehru University, New Delhi 110067, India

Corresponding Author *(Tel: 662- 325-6744; fax: 662-325-1618; email: TMlsna@chemistry.msstate.edu)

Abstract

Commercialization of novel adsorbents technology for providing safe drinking water must consider scale-up methodological approaches to bridge the gap between laboratory and industrial applications. These imply complex matrix analysis and large-scale experiment designs. Arsenic concentrations up to 200-fold higher (2000 µg/L) than the WHO safe drinking limit (10 µg/L) have been reported in Latin American drinking waters. In this work, biochar was developed from a single, readily available, and taxonomically identified woody bamboo species, *Guadua chacoensis.* Raw biochar (BC) from slow pyrolysis (700 ^{o}C for 1 h) and its analog containing chemically precipitated Fe_3O_4 nanoparticles (BC-Fe) were produced. BC-Fe performed well in fixed-bed column sorption. Predicted model capacities ranged from 8.2-7.5 mg/g and were not affected by pH 5-9 shift. The effect of competing matrix chemicals including sulfate, phosphate, nitrate, chloride, acetate, dichromate, carbonate, fluoride, selenate, and molybdate ions (each at 0.01 mM, 0.1 mM and 1 mM) was evaluated. Fe_3O_4 enhanced the adsorption of arsenate as well as phosphate, molybdate, dichromate and selenate. With the exception of nitrate, individually competing ions at low concentration (0.01 mM) did not significantly inhibit As(V) sorption onto BC-Fe. The presence of ten different ions in low concentrations (0.01 mM) did not exert much influence and BC-Fe´s preference for arsenate, and removal remained above 90%. The batch and column BC and BC-Fe adsorption capacities and their ability to provide safe drinking water were evaluated using a naturally contaminated tap water (165 ± 5 µg/L As). A 960 mL volume (203.8 Bed Volumes) of As-free drinking water was collected from a 1 g BC-Fe fixed bed. Adsorbent regeneration was attempted with $(NH_4)_2SO_4$, KOH, or K_3PO_4 (1 M) strippers. Potassium phosphate performed the best for

BC-Fe regeneration. Safe disposal options for the exhausted adsorbents are proposed. Adsorbents and their As-laden analogues (from single and multi-component mixtures) were characterized using high resolution XPS and possible competitive interactions and adsorption pathways and attractive interactions were proposed including electrostatic attractions, hydrogen bonding and weak chemisorption to BC phenolics. Stoichiometric precipitation of metal (Mg, Ca and Fe) oxyanion (phosphate, molybdate, selenate and chromate) insoluble compounds is considered. The use of a packed BC-Fe cartridge to provide As-free drinking water is presented for potential commercial use. BC-Fe is an environmentally friendly and potentially cost-effective adsorbent to provide arsenic-free household water.

Keywords: bamboo biochar, Latin America, arsenic, breakthrough, competitive, XPS, iron leaching

1- Introduction

Arsenic ranks 20th in abundance in the Earth's crust [1]. Arsenic (As) in soils, sediments, and groundwater mainly occurs in pentavalent and trivalent oxidation states [1]. The primary source of As in natural waters is geogenic because As is mobilized by natural geochemical processes [2]. Drinking groundwater contaminated with natural sources of As is believed to be a major source of human exposure [3]. Excessive and prolonged exposure to drinking water containing As may cause numerous health consequences because of its mutagenicity, teratogenicity, and carcinogenicity [4-6]. Dermatitis, skin, lung and bladder cancer, neurotoxicity, hypertension, cardiovascular and respiratory diseases, and Mellitus

diabetes [7-9] are among the many health consequences associated with chronic inorganic As exposure.

The human right to safe, clean, accessible and affordable drinking water has been recognized in 2010 by the United Nations General Assembly (Res. 62/292). However, the contamination of drinking water with As constitutes a global menace with high impact on the poorest regions of the world [4-6]. In South America, about 14 million people drink As contaminated [>10 μg/L[10]] water [11], turning arsenic contamination into a primary public health concern. At low concentrations, arsenate is tasteless, colorless and odorless and the practical difficulty of directly correlating health effects with As intoxication has allowed this problem to be neglected for years [3, 7, 12].

Expensive and/or multi-step treatment technologies, such as reverse osmosis, coagulation and filtration, ion-exchange resins, are known to provide safe As-free water [12-14]. As a result, the treatment of arsenic-contaminated water is of concern to small communities in rural areas around the world, where untreated groundwater is the main source of drinking water. These are often low-income communities that lack access to water supplies, and their inhabitants are mostly unaware that an arsenic problem exists [14, 15]. Small scale, household level, low-cost treatments have been assessed. Among these, heterogeneous photocatalytic [16], bioremediation [17], phytofiltration [18], in situ-remediation using permeable reactive barriers [19], geological materials such as natural adsorbents [11], or engineered biochars [20-22], have been explored. However, there is no universal method available when assessing appropriate technologies for small communities in rural areas. The choice depends on the physicochemical and microbiological composition of waters to be treated [4, 14]. In addition, cheap, easy-to-use, eco-friendly technologies necessarily rely on locally available materials [12, 14].

Functionalizing an adsorbent for aqueous pollutants remediation primarily requires screenings in mono-element aqueous systems. This screening involves dose/volume, pH dependence, kinetics, isotherms and column studies. Results including fast kinetics and/or high adsorption capacities and/or regeneration abilities are the basic needed performance characteristics which at first glance manifest the eligibility of an adsorbent for the screened purpose [23]. Different carbonaceous-based adsorbents demonstrated potential eligibility for pollutants remediation such as for heavy metals [24, 25], oil spills [26], pharmaceuticals [16] and aromatic organic compounds [27]. To bridge the gap between lab results and industrial applications further scalability performance tests are needed. Comprehensive multi-component testing, sorption experiments in natural pollutant concentration media, real water tests and large-scale column tests should be assessed. Very recently Singh et al. [28] presented a mechanistic study at low As(III) concentrations (50–1000 μg/L) to demonstrate sorptive As(III) removal at concentrations usually present in the actual water bodies.

Guadua chacoensis (Rojas Acosta) Londoño & P. M. Peterson [29] is a woody bamboo (Poaceae, Bambusoideae, Bambuseae) native of South America growing in southeastern Bolivia, Paraguay, Brazil, Uruguay and Argentina. It grows in marginal and gallery forests [30, 31]. Its foliage leaves have been proposed as forage (Panizzo et al., 2017), and their mature culms used in construction and crafts [32, 33]. Alchouron et al. (2020) reported that *G. chacoensis* young discarded culms are suitable for biochar synthesis, transforming this valueless waste into biochar adsorbents and iron-oxide dispersants for arsenate removal. This enabled a productive use of the widely available and otherwise wasted clumps.

The aim of this work was to systematically study arsenic removal from polluted drinking water by Fe_3O_4 nanoparticles dispersed on *G. chacoensis* bamboo biochars from a technology transfer.

These goals take into account the following:

1- Applications of modified/engineered biochars are lacking in Latin America [12]

2- Native plantations are beneficial for biodiversity restoration and environmental health [34]

3- *G. chacoensis* bamboo is a wide ranging South American native species whose interest for its sustainable exploitation has grown over the years with increasing knowledge of its uses [32, 33, 35, 36]

4- Fe_3O_4/*G. chacoensis* bamboo biochar composites demonstrated remarkable As(V) Langmuir adsorption capacities (39-868 mg/g), and robust removal over a 5-9 pH window [37]

5- Systematic experiments are needed to design scaled-up technologies for large-scale implementations [12]

Large scale fixed-bed column sorption at different pH's (5, 7 and 9), breakthrough curve modelling capacities, and bed regenerations employing three As aqueous stripping agents (ammonium sulfate, sodium hydroxide and potassium phosphate) were quantified. Two adsorbents were employed, raw *G. chacoensis* biochar (BC) and its BC-Fe analogue containing chemically co-precipitated Fe_3O_4 nanoparticles dispersed on the biochar surfaces. The effect of competing ions on As(V) adsorption was studied in the presence of other anions (sulfate, phosphate, nitrate, acetate, chromate, molybdate, selenate, carbonate, fluoride and chloride) at three different concentrations (0.01, 0.1 and 1 mM). The percent removal of each ion, and the ability to provide safe drinking water from naturally As-

146 contaminated waters was also assessed. Both batch and fixed-bed column remediations
147 were investigated. A comprehensive XPS study was performed to provide a better
148 understanding of competitive surface sorption mechanisms.
149
150 **2. Experimental**
151
152 **2.1. Materials**
153
154 All chemicals used were either GR or AR grades purchased from Sigma Aldrich
155 (Saint Louis, MO). A 1000 mg/L As(V) stock solution of was prepared by dissolving
156 $HAsNa_2O_4 \bullet 7H_2O$ in deionized water. As(V) concentrations were determined using an
157 Inductively Coupled Plasma Mass Spectrometer (ICP-MS), Perkin Elmer SCIEX -ELAN
158 DRC II. Working solutions were freshly prepared before use by diluting the stock solutions
159 with deionized water, and the pH was adjusted to desired values with 0.1 M HCl or 0.1 M
160 NaOH (Hanna HI 2211 pH/ORP Meter). Disposable polypropylene funnels with Whatman
161 No. 1 filter paper were used to separate biochar from solution mixtures.
162 Bamboo-based biochar composites prepared from *G. chacoensis* clumps were used
163 in this study. Fragments (~45 cm from the base) were trimmed from growing discarded
164 young culms. These culms lack commercial value since they naturally crack and dry and
165 are specifically removed by producers to encourage wider culms in the growing clump.
166 Samples were obtained from three different geographic regions in Argentina: Corrientes
167 (Capital department); Corrientes (Empedrado department); and Buenos Aires (Botanical
168 Garden of the Agronomy Faculty of the University of Buenos Aires).

A previous study showed that ultra-high surface area is not required in a biochar for high arsenic sorption [37]. Therefore, expensive and time consuming chemical activation was not done as a pre-treatment. Raw *G. chacoensis* biochar (BC) and its chemically co-precipitated iron-nanoparticle dispersed analogue (BC-Fe) were synthesized following the same protocol as described by Alchouron et al (2020). Briefly, room temperature dried, 0.5 - 1 cm milled particles of *G. chacoensis* culms were subjected to a slow pyrolysis carbonization [700 ^{o}C (10 ^{o}C/min), held for 1 h and cooled to ~25 ^{o}C] under a N_2 atmosphere (10 mL/min), in a tubular muffle furnace (O.R.L, Argentina) inside a steel reactor (AISI 310). The resulting BC (S_{BET} 6.7 m^2/g) was ground, sieved to particle size range of 5-1 mm, and stored in hermetic plastic bags. Pyrolysis temperature was chosen based on prior knowledge of this bamboo charcoal's specific surface area development versus temperature [38].

Magnetite nanoparticle deposition onto BC was performed following a proven method [39]. Solutions of Fe(III) and Fe(II) were prepared separately by dissolving $FeCl_3$ (~100 g) in ~3.9 L distilled water and $FeSO_4$•$7H_2O$ (~160 g) in ~0.45 L of distilled water with stirring for 15 min at ~25 ^{o}C. Solutions were combined, agitated (200 rpm) at ~60 ^{o}C for 15 min, then slowly added into a 150 g BC suspension while stirring (50 rpm) for 30 min at ~25 ^{o}C. Mixture pH was raised to ~10 by adding ~0.15 L of 10 M NaOH dropwise. The mixture was then stirred (50 rpm) for 1 h and aged at room temperature for 24 h. The resulting Fe_3O_4/BC hybrid (BC-Fe-S_{BET} 28.9 m^2/g) was thoroughly vacuum-filtered and washed with distilled water, followed by three ethanol washes, and drying overnight at 70 ^{o}C. The pH of the distilled water washings was monitored until it stabilized at 6.9. During the experiment period, both BC and BC-Fe were stored in glass beakers inside a hot air oven at 70 ^{o}C. The main characteristics of BC and BC-Fe, i.e., Brunauer–Emmett–Teller

(BET) surface area, point of zero charge (PZC), and ultimate and proximate analysis were included in Alchouron et al (2020). The resulting Fe_3O_4/BC hybrid contained wt. 74.2 % Fe_3O_4 and 25.7 wt. % (See supplementary material).

2.2. Artificial As(V)-water sorption studies

2.2.1. Large-scale column breakthrough studies

Fixed-bed continuous flow adsorption studies were conducted and breakthrough curves were constructed to assess the potential of BC-Fe in scaled-up applications [40, 41]. Solution pH on column sorption performance was evaluated at pH 5, 7 and 9, covering the pH range of most As-contaminated underground waters [42].

Three columns (*i.e.*, one for each pH solution) were packed in 3 cm internal diameter glass burettes, using a warm aqueous mixture of 18 g of BC-Fe (15 cm height). Columns were top pressurized at 1.1 bar to maintain a 4 mL/min steady flow (2.26 BV/h). 8 L of a 100 mg/L As(V) solution was passed through each column at 25 ^{o}C. Elute was collected in 200 mL allotments and examined for arsenate concentration. Packed bed breakthrough curves were used to determine the volume of effluent treated, the column exhaustion point and the pH effect on these variables. The bed volume (BV) was calculated from the expression [43]:

$$\text{Bed volume} = \pi R^2 \text{h}$$

where R is the radius of the column and h is the bed height.

2.2.2. Effect of competing ions in water studies

Ions present in natural waters may compete with arsenic for adsorption [44-46]. As(V) adsorption onto BC and BC-Fe was investigated in the presence of sulfate, phosphate, nitrate, chloride, acetate, dichromate, carbonate, fluoride, selenate and molybdate. These ions were selected based on the following criteria: similar chemistry to arsenate (phosphate, dichromate, selenate, molybdate and sulfate) and their typical presence in natural waters (nitrate, chloride, acetate, carbonate and fluoride). The effect of each ion was explored at three different concentrations (0.01, 0.1 and 1 mM) with 10 mg/L As(V) [0.07 mM of AsO_4^{3-}]. Then, the simultaneous effect of all 10 ions on arsenic adsorption was studied at three different concentrations (each ion is present at 0.01, 0.1 or 1 mM) to three separate solutions containing 10 mg/L As(V) [0.07 mM of AsO_4^{3-}]. In all cases, experiments were done in triplicate with 50 mg of adsorbent (BC or BC-Fe) in 25 mL solutions at 25 ^{o}C, for 2 hrs while mixing at 300 rpm. Post agitation mixtures were separated by filtration and remaining arsenic concentrations were quantified.

To better understand competitive adsorption, ions remaining in solution after adsorption were quantified using atomic absorption (chromium), ICP-MS (molybdate and selenate), ion selective electrodes (chloride and fluoride), liquid chromatography UV-Vis (nitrate) and UV-Vis (phosphate). Sulfate, acetate and carbonate where not determined due to unavailability of suitable analytical equipment.

2.3. As-contaminated domestic water sorption studies

Arsenic (0.17 ± 0.01 mg/L) contaminated water was collected from a domestic faucet in Altamirano (35°21'46.2"S, 58°09'18.8"W), Buenos Aires, Argentina. Prior to collection, the faucet was open to continuous water flow for 3 min. The sample was collected in plastic bottles, hermetically sealed, and stored at -4 ^{o}C for transport and during the experimentation.

2.3.1. Batch studies

Arsenic adsorption by BC and BC-Fe, was determined for this domestic water. The biochar dose (0.01 to 0.5 g) and the biochar/solution contact temperature (5, 25 and 40 ^{o}C) were simultaneously evaluated in triplicate. Biochars were equilibrated with 50 mL of water at 300 rpm for 120 min. Experiments were done in triplicate and standard error bars were included in all plots using the standard deviation of these replicates.

2.3.2. Column studies

A BC-Fe fixed-bed continuous flow arsenic breakthrough curve was obtained to evaluate the dynamic behavior of the adsorbent in As-contaminated domestic water. The column was packed in a 1 cm internal diameter glass burette using a warm mixture of distilled water and 1 g of BC-Fe (6 cm height). A total volume of 8 L of water was passed through the column at 25 ^{o}C at a steady flow of ~ 4 mL/min (50.9 BV/h). Samples were collected in 150 mL allotments and examined for arsenic. Based on BC´s capacity and results in section 2.3.1, experiments were not performed on BC.

2.4. Adsorbent regeneration and iron leaching studies

Regeneration of BC and BC-Fe were studied by equilibrating the As-laden biochars with three aqueous stripping agents separately: ammonium sulfate, potassium hydroxide and potassium phosphate. Biochars were first loaded in batch experiments with arsenic solutions (50 mL of 100 mg/L As(V)) and were equilibrated (300 rpm, 1 h) at pH 7 with 0.1 g of biochar at 25 ^{o}C. Batch desorptions were carried out by stirring (300 rpm, 12 h) the As-laden BC and As-laden BC-Fe with 50 mL solutions of each stripping agents at 1M. Sorption-stripping cycles were performed three times. Filtrates were analysed for arsenic and mass balance was used to quantify the amount of arsenic adsorbed or desorbed.

Iron dissolution from BC-Fe was studied by completing three batch sorption equilibria (1 g of BC-Fe, 50 mL of 1000 mg/L As(V) at 25 C, vortex shaking for 2 mins) and then stripping (1 g of BC-Fe, 50 mL of 1000 mg/L As(V) at 25 C, vortex shaking for 2 mins) with 1 M potassium hydroxide, potassium phosphate, sodium hydroxide, and sodium chloride. Filtrates were analyzed for iron using a Shimadzu AA-7000 Atomic Absorption Spectrophotometer (AAS). Experiments were done in triplicate and standard error bars were included in all plots using the standard deviation of these replicates.

2.5. Characterisation

2.5.1. X-ray photoelectron spectroscopy (XPS)

X-ray photoelectron spectroscopy (XPS) analyses were run on a Thermo Scientific K-Alpha XPS system with a monochromatic X-ray source at 1486.6 eV, corresponding to the Al K_{α} line, with a spot size of 400 μm^2. Photoelectrons were collected at a takeoff angle

of 90^0 relative to the overall sample's fractal particle surface. Measurements were made in the constant analyzer energy mode. The survey spectra were taken at a pass energy of 200 eV. High resolution (HR) core level spectra were taken at a 40 eV pass energy. The XPS data acquisition were performed using the "Avantage v5.932" software provided with the instrument.

2.5.2. Magnetic moment

Magnetic hysteresis measurements were carried out on a Lake Shore 7304 Vibrating Sample Magnetometer (VSM). The magnetic properties of the adsorbents are represented by plots of magnetization (*M*) against the field strengths (*H*) giving the hysteresis loop. The saturation magnetization was measured from the hysteresis curve.

3. Results and discussion

3.1. Simulated As(V)-water sorption studies

3.1.1. Large-scale column breakthrough studies

The fixed bed column performance for arsenates removal depends on the column's capacity as a function of initial adsorbate characteristics, flow rate, and bed height [47]. For the three As(V) solutions (pH 5, 7 and 9), the As(V) retained (mg/g) in the column was determined by mass balance calculations and integrating the breakthrough curve area (from t_0 to t_t) obtained by plotting the concentration ratio (C/C_0) versus flow time (min) (Figure 1.a). The breakthrough time (t_u) is defined as, C/C_0 being ~ 0.01 (1%) of the influent and the equivalent to 0.01 mg/L of As(V) eluted, which coincides with the WHO's maximum permissible arsenic limit. The bed volume (BV) of the fixed bed was of 106 mL. Thus, the steady 4 mL/min flow rate is equivalent to a 2.3 BV/h. Complete saturations of the bed

306 occurred after 27, 35, and 25 BV for pH 5, 7 and 9, respectively. The predicted model
307 capacities were 8.2, 8.4 and 7.5 mg/g for pH 5, 7, and 9, respectively. Results were then
308 verified by mass balance calculations. Complete column performance descriptions are
309 presented in Table 1. The pH influenced capacities only slightly [(3.9 mg/g (mass balance
310 calculations) or 1.0 mg/g (breakthrough curve integration)]. Previous *G. chacoensis's* BC-
311 Fe´s batch adsorption studies were also not significantly affected within the pH (5-9) range
312 [37] .

313 The ratio between time equivalent to usable capacity and time equivalent to total
314 stoichiometric capacity ($t_u/t_t = H_b/H_t$) is the fraction of the total bed capacity or length
315 utilized up to the breakthrough point. Hence, the bed length of H_t, H_b is the length upon
316 reaching the breakpoint [40]. Usable bed lengths varied with 5-9 pH between 8.7 to 11.3
317 cm (Table 1). When the polluted water is initially passed through the inlet of the column,
318 the mass transfer zone is accomplished by the upper layers of the fresh adsorbent [48]. At
319 this point $C/C_0 = 0$. While feeding the As(V) further into the column, the sorbent sorption
320 sites gradually saturate, and the mass transfer zone travels, descending to un-adsorbed
321 zones [48]. At the breakpoint, the fractions of the total bed capacities used were 0.3 (pH =
322 5), 0.4 (pH = 7), and 0.3 (pH = 9). When the effluent concentration is close to the inlet
323 concentration [(C/C_0)~1.0] the breakthrough occurs, the bed is judged to be ineffective,
324 and regeneration is required.
325

Table 1. Fixed-bed continuous flow column test data for BC-Fe at pH 5, 7 and 9 and at 25 °C.[a]

	Breakthrough point (min)	Saturation point (min)	Bed volumes until saturation (BV)	Column capacity by breakthrough curve integration (mg/g)	Column capacity by mass balance calculation (mg/g)	Usable column length (cm)	Unusable column length (cm)
pH 9	214	660	25	8.2	7.2	10.1	4.9
pH 7	395	935	35	8.4	11.2	8.7	6.3
pH 5	178	711	27	7.5	8.0	11.3	3.7

[a]Tests were carried out on 18 g of BC-Fe packed fixed-bed (15 cm) columns at 25°C, pressurized at 1.1 bar. A total volume of 8 L of a 100 mg/L As(V), pH 5, 7 and 9 solution, was passed through the column at an average flow of 4 mL/min.

Robust initial As(V) uptake was achieved by the fixed-bed column contacted with the As(V) solution at pH 7 versus pH 5 and 9, and then rapidly decreased as the saturation point is reached. At these experimental conditions, the column which the As(V) solution at pH 7 had passed through, would achieve 1580 mL safe arsenic water (As<10 µg/L) up to the column breakpoint, and by that time, BC-Fe would be laden with 0.5 mg/g of arsenic.

Previous experiments evaluating BC-Fe´s column performance at pH 7 gave a column capacity of 10.2 mg/g from mass balance [37], while this current work showed an 11.2 mg/g capacity. The inlet concentration (100 mg/L) and temperature of contact (25 °C) were similar in both experiments. Flow rate and column-heights were 3.4 times faster (from 1.18 to 4 mL/min) and 3 times longer (from 6 cm to 18 cm). It was presumed that this chosen flow rate might have sharpened the breakthrough curve since the residence time of the sorbate in the column was not long enough to reach equilibrium. However, the height increase possibly compensated for this by increasing the sorption site density. Hence, the increasing amount of BC-Fe leads to a longer adsorbate/ adsorbent interaction time.

346 **Table 2.** Comparison of fixed-bed column capacities with batch sorption capacities at 25 °C.

Carbonaceous adsorbent	C_{inlet} mg/L	Flow rate mL/min	pH	Column capacity calculates by mass balance mg/g	Column model predicted capacity Model	mg/g	Batch Langmuir capacity mg/g	Batch/column capacities**	References
Al-enriched Tetra Pak biochar	135	1	3	18.3	Thomas	15.8	33.2	2.1	[49]
Fe-impregnated biochar	50	2	5.8	0.83	n/s	n/s	2.16	2.6[a]	[50]
Thioglycolated sugarcane carbon	0.0015	3	6	0.08183	Thomas	0.083	n/d	n/s	[51]
Fe-mixed mesoporous pellet	0.5	17	5		Thomas	0.43	5.4	12.6	[52, 53]
Iron oxide nanoneedle array-decorated biochar fibers	0.275	2.26	6.7	n/s	Bed volumes	n/s	93.94	n/d	[54]
Fe-Mn Granular activated carbon	0.12	6	8.2 2	n/s	Thomas	34	2.3	0.1	[55]
Fe impregnated granular activated carbon	0.25	10.8	n/s	0.47	n/s	n/s	1.43	3.0 [a]	[56]
Algal derived-biochar	25.00	5	n/s	8.12	Thomas	8.16	7.67	0.9	[57]
Crawfish shell biochar	80	5	n/s		Thomas	2.85	17.2	6.0	[58]
Bamboo Fe-biochar	100	1.18	7	10.2	Breakthrough curve integration	13.9	89.9	6.5	[37]
Guadua chacoensis Bamboo Fe-biochar	100	4	9	7.23	Breakthrough curve integration	8.2	n/s	n/s	This study
			7	11.2		**8.4**	**90**	10.7	
			5	7.99		7.5	n/s	n/s	

347 *n/s= not specified. ** Calculated between the Langmuir and the model-predicted capacities for exception of (a) which were
348 calculated between Langmuir and mass-balance capacities since model-predicted capacityes were not determined [= batch Langmuir
349 capacity / column capacity].

Column sorption data using carbonaceous sorbents for aqueous As(V) removal are presented in Table 2. Initial adsorbate concentration (C_{inlet}), flow-rate, and pH were reported for the best column performance capacity in each study. Higher C_{inlet} values resulted in earlier breakthrough and exhaustion times [48]. Increased inlet concentrations generate a higher driving force to overcome mass-transfer resistance in the liquid phase, and the adsorption sites are more quickly exhausted. This reduces the volume of the treated effluent, but no direct relationship can be established between inlet concentration and column capacity (Table 2). Nikic et al. studied a Fe-Mn granular activated carbon at 0.12 mg/L As(V) C_{inlet} at a relatively fast flow rate (6 mL/min). This gave a high 34 mg/g column capacity. Ding et al studied Al-enriched Tetra Pak biochar at a 135 mg/L C_{inlet} and a relatively slow flow-rate (1 mL/min) resulting in a 15.8 mg/g arsenic column capacity [49, 55].

The reported Fixed-bed-Column-Capacity versus Batch-Langmuir-Capacity ratios are shown in Table 2. With the exception of Nikic et al, fixed-bed capacities decreased to 12.6 times the batch sorption capacities. Senthilkumar et al reported similar capacities on algal-derived biochar due to its rapid kinetics (< 30 min) [57]. Nikic et al reported a surprise capacity increase from 2.3 mg/g (in batch studies) to 34 mg/g (in column studies) [55]. However, the isotherm data was obtained for low (0.1-1 mg/L) arsenic concentrations. A higher Langmuir capacity would probably have been obtained at higher concentrations.

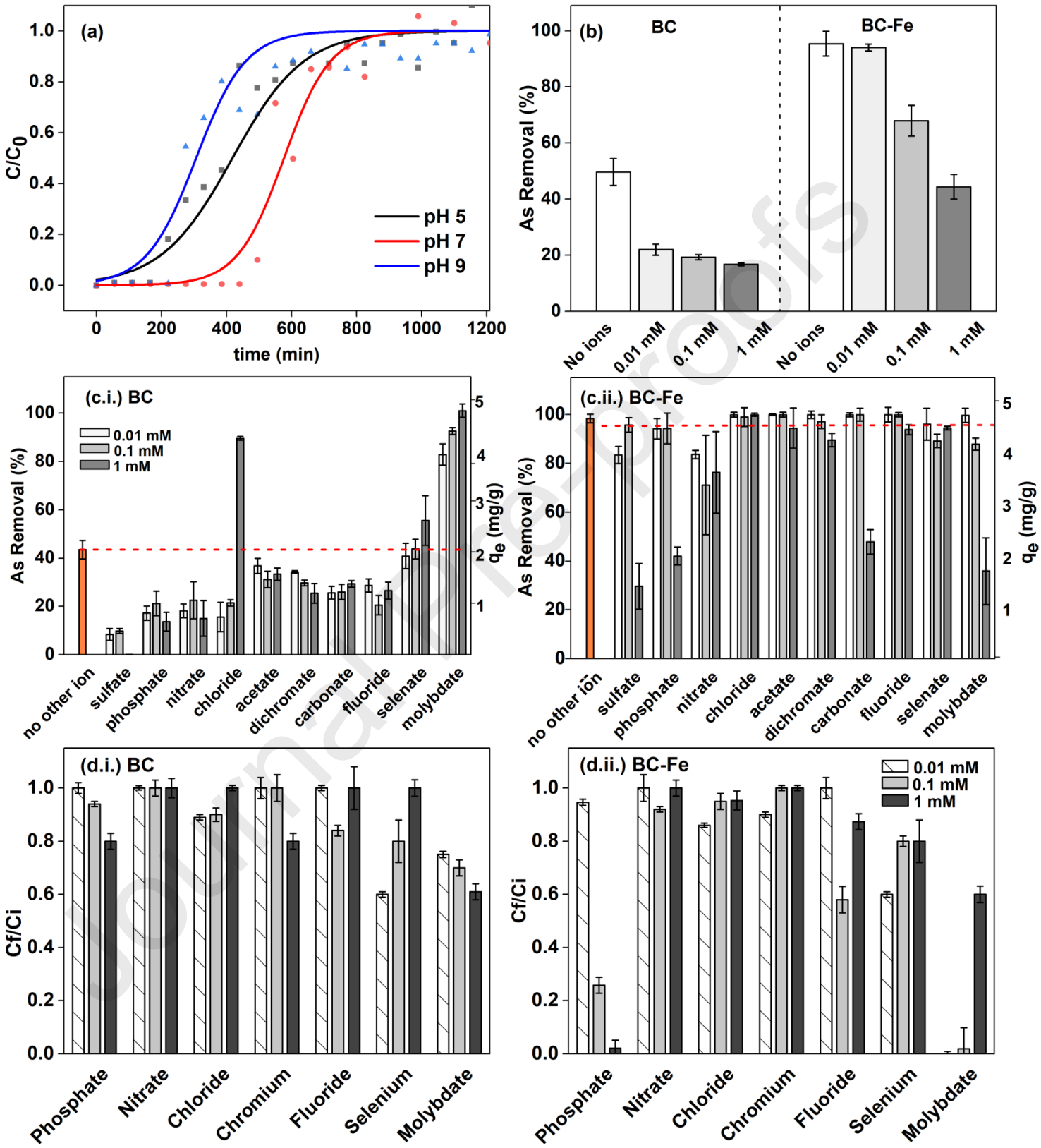

371 **Figure 1. (a)** Continuous flow fixed-bed column breakthrough curves for As(V)

adsorption onto BC-Fe at pH 5, 7 and 9. C is the effluent concentration at time t (min) and C_0 is the influent concentration (mg/L). Each column contained, 18 g of BC-Fe (15 cm height) packed in 3 cm internal diameter glass burettes. A 4 mL/min (2.26 BV/h) steady flow of a 100 mg/L As(V) solution was passed through each column at 25 ^{o}C. **(b)** The simultaneous effect and **(c)** the individual effect of 10 ions (sulfate, phosphate, nitrate, chloride, acetate, dichromate, carbonate, fluoride, selenate and molybdate) on As(V) aqueous adsorption by BC or BC-Fe. The adsorbent's capacity (q_e) is expressed as the mg of As(V) adsorbed by a g of biochar. Three different competing ion concentrations were used (0.01, 0.1 or 1 mM) in three separate 10 mg/L As(V) solutions, 50.0 mg dose of adsorbent, 25 ^{o}C, 300 rpm agitation and 2 h equilibration. The red dotted line is traced based on the control 'no ion' treatment. **(d)** Quantification of competitive ions individually after contacting each with BC and BC-Fe at three different concentrations (0.01, 0.1 and 1 mM) in a 10 mg/L aqueous As(V) solution. (d.i.) on BC and (d.ii.) on BC-Fe (50.0 mg dose of adsorbent, 25 ^{o}C, 300 rpm agitation and 2 h equilibration). C_f/C_i is the ratio of the final (C_f) over the initial (C_i) concentration. **(b-d)** Error bars are standard deviations of three repetitions.

3.1.2. Effect of competing ions on As(V) removal from water

BC's and BC-Fe´s arsenate removal was robust at natural water pH (5-9) [37]. Arsenate removal on water treatment will mainly vary with the existence of competing ions present in surface and ground waters. BC and BC-Fe are both multiphase adsorbents with three or four phases (*i.e.*, biochar, silica, minerals like $CaCO_3$ and magnetite) that can interact with other ions. An in-depth understanding is needed to systematically design adsorbents for water treatment. Figure 1.c displays the effect of ten individually competing

ions at low, medium and high concentrations (0.01, 0.1 and 1 mM, respectively) on As(V) removal from aqueous 10 mg/L As(V) solutions by (c.i.) BC and (c.ii.) BC-Fe. In the absence of any competing anions in water, BC-Fe´s As(V) equilibrium uptake was complete (98% ± 1.7), while BC´s sorption was 43 % ± 3.8 under conditions summarized in the figure 1.c caption.

Each competing anion either enhanced or decreased arsenate uptake on BC. MoO_4^{2-}, for example, increased As(V) uptake on BC. As(V) removal rose as molybdate solution concentration increased. This could be due to the increased ionic strength of the solution. Arsenate adsorption was being boosted by the time molybdate was also being retained (Figure 1.d.i.). High chloride concentrations also enhanced As(V) sorption on BC. The chloride solutions were prepared using magnesium chloride. It is possible the Mg^{2+} deposited on the biochar surface or in solution was responsible for forming a water insoluble stoichiometric magnesium arsenate compound like $Mg(HAsO_4)_2$ or $(Mg_3(AsO_4)_2$ [Ksp = 8.16×10^{-22}] [59]. This was further verified with the XPS low resolution survey spectra (Table S2) and further discussed in supplementary material (section 4). Similar observations were reported by Fang [60] and Jiang, Chu, Amano and Machida [61] for phosphate sorption in the presence of Mg^{2+}.

Sulfate, phosphate, nitrate, acetate, dichromate, carbonate and fluoride decreased BC´s As(V) uptake. Interestingly (with exception of sulfate), with the increase of ion concentration from 0.01 to 1 mM, the arsenic removal remained unchanged. Presence of sulfate strongly affected the immobilization of As(V) sorption on BC. A 0.01 mM of sulphate had the same effect as 1 mM of phosphate or nitrate. The presence of SeO_4^{2-} in the solution did not affect As(V) sorption.

Iron-oxide nanoparticles deposited BC (BC-Fe) exhibited different trends in competitive sorption. The presence of Cl^- and CH_3COO^- in solutions did not influence the As(V) sorption. In addition, $Cr_2O_7^{2-}$, F^- and SeO_4^{2-} showed negligible effects on arsenic sorption i.e., ~ 3 % decrease only at high ion concentrations. The point of zero charge (PZC) for BC-Fe is ~ 4 and surface is negatively charged at the pH used in these experiments (pH = 7). Higher electrostatic repulsion with negatively charged deprotonated Fe_3O_4 surface hydroxyls may occur at pH 7-9. With the exception of nitrate, low concentration of ions (0.01 mM) did not show any significant As(V) sorption inhibition. At a 1 mM competing ion concentration, the order of BC-Fe´s As(V) sorption drop was $SO_4^{2-} = MoO_4^{2-} = PO_4^{3-} \geq CO_3^{2-} > NO_3^- > Cr_2O_7^{2-} > F^- = SeO_4^{2-}$. In the presence of 1 mM sulfate, As(V) uptake dropped dramatically to ~ 30 %. Molybdate, phosphate and carbonate (1 mM) dropped As(V) sorption to ~40, 40 and 45% respectively. The quantifications of MoO_4^{2-} and PO_4^{3-} carried out after sorption are shown in section 3.1.2.2. At high concentrations' competition exist for sorption sites. Sulfate, molybdate and phosphate are tetrahedral oxyanions as are arsenates and form inner-sphere chemisorbed complexes with surface hydroxyl groups of deposited magnetite on BC-Fe [62-64].

The effect of the simultaneous presence of ten competing ions mixed together at three different concentrations on the removal of 10 mg/L aqueous As(V) solution for BC and BC-Fe is presented in figure 1.b. The presence of the ten ions even at 0.01 mM, strongly affected BC's As(V)´s sorption, lowering the removal from ~50% to ~22% under conditions summarized in section 2.2.2. However, the increasing concentration (from 0.01 to 1 mM) and thus the increasing ionic strength of the system did not seem to have a significant effect on sorption. The same trend (the robust maintenance of the arsenic

441 removal despite the increasing concentration of ions) was observed for single ion
442 competitive experiments (Figure 1.c.i.). In contrast, the presence of ten ions in low
443 concentrations (0.01 mM) did not significantly influence BC-Fe´s preference for arsenate,
444 and removal remained above 90% (Figure 1.b.). Subsequently, arsenate removal decreased
445 to 50% in the presence of ten ions in high concentrations (1 mM).

446 All in all, the influence over arsenic uptake in the presence of ions for BC is higher
447 than for BC-Fe. Although, they are both multiphase adsorbents, BC-Fe is dosed with
448 magnetite particles with surface iron hydroxyls. This adsorbent phase has higher affinity for
449 anion adsorption than that of carbonaceous char and silica dominantly present in BC [65,
450 66]. Magnetite particles, which serve as sorption sites, increase the surface for electrostatic
451 interactions that may generate stronger As-interactions in BC-Fe versus BC [21]. The
452 nature of As(III/V) chemisorption on magnetite has been carefully studied [20, 67]. In
453 addition, BC-Fe's As(V) Langmuir adsorption capacity is higher than that of BC (90 and 49
454 mg/g, respectively) [37]. Thus, the relative contribution of each competitive ion over As-
455 removal by BC compared with BC-Fe is almost 1:2. The competitive effect of dissolved
456 anions in water must be taken into account when designing an effective arsenic treatment
457 system.

458 Competitive ion adsorption [in 10 mg/L As(V)] was quantified after stirring with
459 batch suspensions of BC or BC-Fe. The results of these quantifications are shown in figure
460 1.d. BC did not remove nitrate, chloride and fluoride. Phosphate and chromium were
461 slightly removed at high ion concentrations. Molybdate was partially removed and upon
462 increasing its concentration (from 0.0 to 1mM), and its uptake rose (Figure 1.d.i.) as did
463 that of arsenate (Figure 1.c.i.).

464 Both BC and BC-Fe removed phosphate and molybdate (Figure 1.d.). Arsenate,
465 molybdate and phosphate anions have a similar geometry and compete for the same
466 adsorption sites [20, 63, 64]. Competitive phosphate sorption with arsenate has been
467 reported for many types of adsorbents [50, 68]. Nitrates, fluoride and chlorides have lower
468 affinities for magnetite surface hydroxyls as their adsorption occurs primarily through
469 hydrogen bonding [69]. The possible sorption interactions of the competitive contaminants
470 and arsenic on BC and BC-Fe surfaces are further discussed, proposed and schematized in
471 section 3.4 and supplementary material (section 4).
472

473 **3.2. Batch and column studies for arsenic sorption from As-contaminated**
474 **household water onto BC and BC-Fe.**
475

476 Table S1 shows some characteristics of the natural water sample tested in this study.
477 All values of dissolved contents are within safe limits for drinking water with the exception
478 of arsenic (16 times over WHO recommended limit). Adsorption results are systematically
479 discussed considering the physical and chemical characteristics of the sample and the
480 possible interactions discussed in sections 3.1, section 3.4, and supplementary material
481 (section 4). Predictions of the amount of safe drinking water obtained without adsorbent
482 regeneration have been carefully made and are presented in the context of WHO's As (<
483 0.01 mg/L) limit.
484 As(V) batch sorptions on BC and BC-Fe for a naturally As (0.16 mg/L ± 0.02)
485 contaminated tap water using adsorbent amounts from 0.01 to 0.5 g and contact
486 temperatures of 5, 25 and 40 ^{o}C are displayed in figure 2.a. Increasing the adsorbent dose in
487 these 50 mL water samples had no effect on BC's arsenic uptake but increased BC-Fe's.

BC was unable to reduce the arsenic concentration to safe levels or even close to safe levels. However, BC-Fe in a 2 g/L dose (0.1 g of BC-Fe into 50 mL of solution) was sufficient to provide safe drinking water at 40 ^{o}C. In a 5 g/L dose BC-Fe gave safe water at all three temperatures.

The water sample had 58 mg/L (0.6 mM) of sulfate. This concentration is *slightly high* considering the conditions simulated in section 3.1.2. The presence of sulfate dropped As(V)´s uptake by both BC and BC-Fe (Figure 1.c.). Therefore, this level of sulfate may explain the low BC arsenic uptake displayed in figure 2.a.

Sorption of As onto BC-Fe is endothermic. In simulated As-water systems, Langmuir sorption capacities were reported to increase with temperature (90 mg/g at 25 ^{o}C and 457 mg/g at 40 ^{o}C) [37]. Similar trends were observed for BC-Fe at both 1 (0.05 g) and 2 g/L (0.1 g) dose. However, at a dose of 2 g/L (40 °C) the safe drinking water limits have been reached.

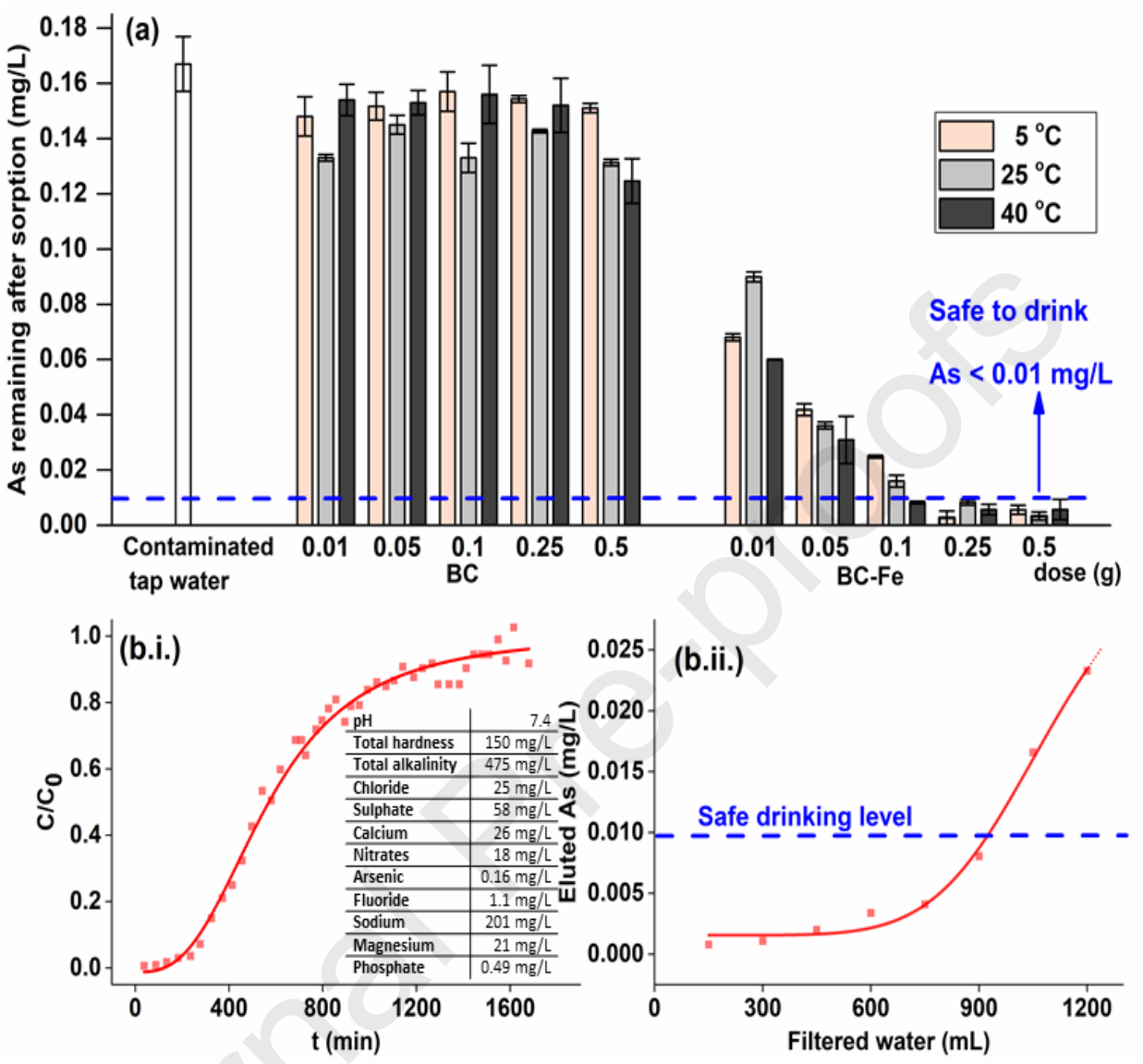

Figure 2. (a) As(V) adsorption on BC and BC-Fe of a naturally As (0.16 mg/L ± 0.02) contaminated water when varying adsorbent amount (0.01-0.5 g) and contact temperature (5, 25 and 40 °C). Biochars were equilibrated with 50 mL of water at 300 rpm for 120 min. Safe to drink water is defined here at 0.01 mg/L of As(V) as recommended by WHO. Error bars are the standard deviation of three repetitions. **(b)** Continuous flow fixed-bed column study of a naturally contaminated As(V) water sample passed at a ~ 4 mL/min flow rate (51 BV/h) onto 1 g of BC-Fe (6 cm bed height, 1 cm inner column diameter,) at 25 °C. (b.i.)

509 Breakthrough curves for arsenate adsorption onto BC-Fe, (b.ii.) A plot showing the arsenic
510 in the water that has eluted from the column (mg/L) versus the mL of filtered water,
511 displaying the safe drinking water guideline for As defined by the WHO (< 0.01 mg/L).
512 The important components of the natural water used in the study is listed in the table inside
513 (Figure 2, b.i.) and the complete water analysis is displayed in Table S1.

514 A fixed-bed continuous flow adsorption study on BC-Fe was conducted to evaluate
515 the dynamic behavior of the adsorbent over naturally As-contaminated household water.
516 Packed bed performance was assessed using a breakthrough curve (Figure 2.b.). A
517 breakthrough point at 0.01 mg/L was established (Figure 2.b.i.) based on the WHO's safe
518 drinking standard. A 960 mL volume of safe As drinking water, equivalent to 203.8 BV,
519 was collected (at the conditions described in section 2.3.2.) by using 1 g of BC-Fe

520 When the eluted arsenic concentration reaches > 0.01 mg/L, the BC-Fe adsorbent
521 must be replaced. Based on the mass balance calculations, 19.5 µg of As/g of BC-Fe would
522 be adsorbed onto BC-Fe at this point. If these residues were to be disposed of, according to
523 the toxicity-specific leaching procedure (TCLP) developed by USEPA [70], there would be
524 less arsenic than the maximum limit accepted (100 times the acceptable limit in drinking
525 water, i.e., 1000 µg/L). Countries such as Argentina [71] rely on this regulation in order to
526 determine whether solid residues (in this case 19.5 µg/g As adsorbed on BC-Fe) are
527 hazardous or not hazardous. Thus, since this is considered a non-hazardous residue, BC-Fe
528 can be disposed of inside a household bin (see supplementary material, section 3).

529 A simple cartridge-based devise for domestic water treatment with this biochar/iron
530 oxide adsorbent with commercial implications appears in the supporting material (Section
531 6). Testing of low-cost designs is underway for home-level arsenic remediation.

532

3.3. Adsorbent regeneration

BC and BC-Fe reusability was studied by conducting three consecutive batch sorption-regeneration cycles using either aqueous ammonium sulfate, aqueous potassium phosphate or aqueous potassium hydroxide as stripping agents (Figure 3.). Biochars were first loaded in batch loadings with arsenic solutions (50 mL of 100 mg/L As(V)) and were equilibrated (300 rpm, 1 h) at pH 7 with 0.1 g of biochar at 25 ^{o}C. After the first adsorption cycle, no As(V) was detected in remaining solution. Hence, BC-Fe adsorbed all arsenic present in the solution used to load the adsorbent for regeneration in the next step (q_{max} of 50 mg/g). The BC adsorbed a total of 15 mg/L (q_{max} of 7.5 mg/g). To compare adsorbents and sorption performance during sorption-regeneration cycles, q_{max} values were considered to be 100 % of the As adsorbed. BC-Fe's and BC's Langmuir arsenic adsorption capacities are 90 mg/g and 49 mg/g, respectively [37]. Regenerations when the maximum adsorbent capacity is not completely As-saturated may be more challenging. The first adsorbent/adsorbate contact occurs at sites where interactions are strong (bidentate) thus not as available for stripping agents to affect their interactions [20, 37].

When employing all three stripping agents over the As-laden BC, the amount of stripped arsenic is low (Figure 3. a-c). In the first cycle, potassium hydroxide managed to strip 37 % of the adsorbed arsenate from BC, while potassium phosphate and ammonium sulphate stripped 20 % and 2 % respectively. Basic pH shift due to hydroxide affected As/BC chemisorption. After the 1st cycle of treatment with either 3 stripping agents, BC's arsenic uptake is reduced to ~ 50 %. Surprisingly, the adsorption percentage is maintained after the 2nd and 3rd cycles. Portions of As get tightly bound and resist stripping, thus

556 reducing As uptake cycle by cycle, but as the capacity of biochar does not collapse, arsenic
557 can still be adsorbed.

558 For BC-Fe, the study carried out using potassium phosphate (Figure 3. e.) as a
559 stripping agent displayed a different trend than that shown when employing ammonium
560 sulfate or potassium hydroxide (Figure 3. d., f.). Potassium phosphate was a superior
561 stripping agent and the ratio of stripped arsenic was 0.8 and 0.5 for 1st and 3rd cycles.
562 Phosphates and arsenates compete for adsorption onto magnetite. Cycle to cycle, portions
563 of As become tightly bound and resist stripping, thus reducing As uptake. Arsenic stripped
564 by ammonium sulphate and potassium hydroxide in the 1st cycle only accounted for ~ 17 %
565 and ~ 10 %, laden As respectively. Although BC-Fe was loaded with all available As in
566 solution (q_{max} of 50 mg/g), it is not its saturation capacity (90 mg/g) and therefore does not
567 prevent the loading of more arsenic. Thus, its Langmuir arsenic adsorption capacity is not
568 reached up to the 2nd cycle and explains As the adsorption decrease in the 3rd cycle.

569 Biochar's application will determine the most appropriate regeneration agent. It is
570 difficult to determine whether BC or BC-Fe are more easily regenerated. In this work, any
571 of the three stripping agents managed a total adsorbents regeneration. This reveals the
572 stability of the As(V)-Fe_3O_4-BC or As(V)-O-BC hybrid adsorbents. The order of % As
573 stripped per stripping agent used is ammonium sulfate < potassium hydroxide < potassium
574 phosphate (Fig. 3. a.,d.). Potassium phosphate is best for BC-Fe. Strong acids or bases like
575 HCl and NaOH proved to be good As stripping agents [72, 73] and should be considered if
576 desiring a complete adsorbate/adsorbents regeneration. However, at highly acidic or basic
577 concentrations, Fe^{2+} and Fe^{3+} can be leached from iron oxides and reduce the ability to use

adsorption/regeneration-cycles. The logic followed in Section 3.2 (TCLP) should be followed.

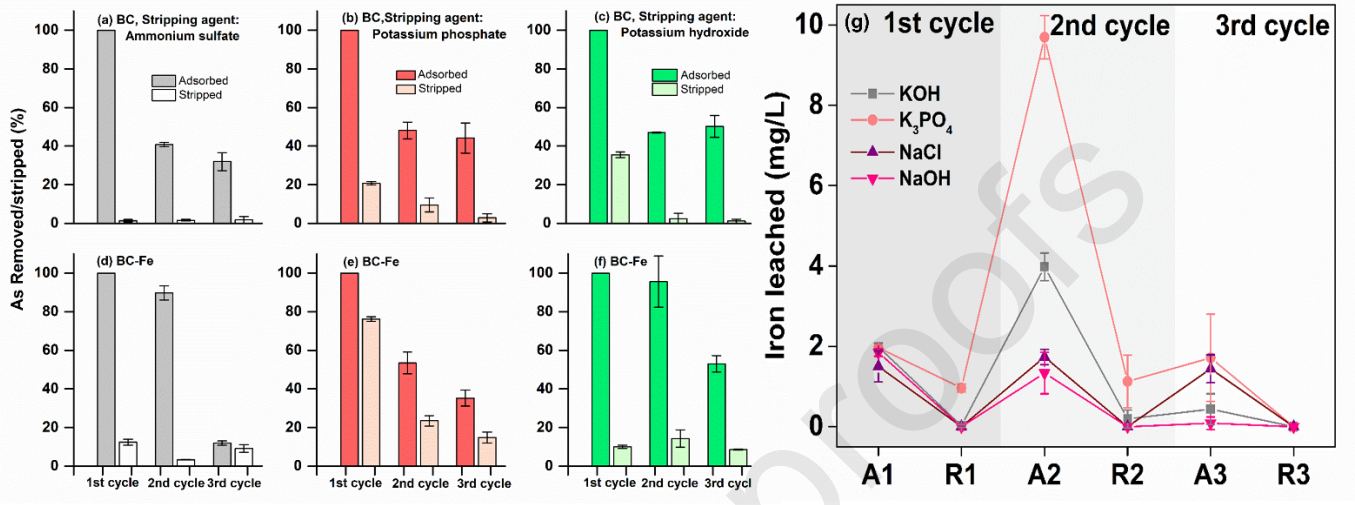

Figure 3. Sorption-regeneration studies: the wt % of As (V) removed from the solution (adsorbed) and stripped from the adsorbent (regenerated) during 3 adsorption/regeneration cycles by BC and BC-Fe using three different 1M stripping agents [ammonium sulfate (a, d), potassium phosphate (b, e), and potassium hydroxide (c and f)]. The 100 % is based on an As adsorption q_{max} of 7.5 mg/g for BC (a-c) and of 50 mg/g for BC-Fe (d-f) and g). Quantification of the iron leached (mg/L) from BC-Fe to the solution is shown during three consecutive adsorption **(A)**-regeneration **(R)** cycles utilizing four different stripping agents: KOH, K_3PO_4, NaCl, and NaOH. Experiments were run in triplicate, at 25 ^oC, equilibrated for 2 min (full speed vortex shaking) using 1 g doses of adsorbent, in 50 mL solutions. As(V) adsorption cycles were performed in a 1000 mg /L solution and desorption (regeneration) cycles in a 1 M solution of each stripping agent. Error bars are for 3 replicates.

Figure 3g displays quantifications of the leached iron (mg/L) from BC-Fe to the solution during three consecutive adsorption(A)-regeneration(R) cycles utilizing four

596 different stripping agents (KOH, K_3PO_4, NaCl and NaOH). Partial dissolution of iron from
597 the sorbent was higher during contact with the high concentration 1000 mg/L-As(V)
598 saturated solution than with the 1M stripping agent solutions in all three adsorption-
599 regeneration cycles. In the 2nd adsorption cycle, the iron leached into the solution
600 previously contacted with K_3PO_4 was 9.6 mg/L. This amount was way greater than the
601 previously contacted with KOH (3.98 mg/L), NaCl (1.7 mg/ L) and NaOH (1.3 mg/ L).
602 Material characteristics were modified more potassium phosphate stripping. This may
603 affect the efficiency of the spent sorbent regeneration. No significant differences existed
604 among the adsorption or among the regeneration treatments in the 3rd cycle´s Iron leaching.
605 Iron leaching in the 3rd regeneration cycle was null. BC-Fe's contact with both NaCl and
606 NaOH solutions had the least effect over iron leaching.

607 In high acid or base solution concentrations, Fe^{2+} and Fe^{3+} are partially leached from
608 iron oxides, reducing the ability to use several adsorption/regeneration cycles. Additionally,
609 stoichiometric As-Fe compounds may be formed and precipitated from the solution and
610 deposition on BC-Fe. This can be intensified in As saturated concentrations. Experiments
611 exploring iron leaching from the sorbents with different As concentrations will be further
612 assessed.

613 **3.4. XPS characterization, adsorption pathways and mechanisms**

614 XPS probed the elemental composition and oxidation states of the BC and BC-Fe
615 surface regions after sorption of multi-ion mixtures at 0.01, 0.1 and 1 mM. These mixtures
616 contained sulfate, phosphate, nitrate, chloride, acetate, dichromate, carbonate, fluoride,
617 selenate, and molybdate. The high resolution XPS As2p, Cr2p, Se3d, Mo3d, and P2p spectra
618 obtained were each deconvoluted; peaks were assigned and displayed in figures 4, S3-S7.

619 Their binding energies, atomic percentages and FWHMs are presented in Table S3. XPS
620 write up, deconvolution and interpretations are presented in supplementary material (section
621 4).

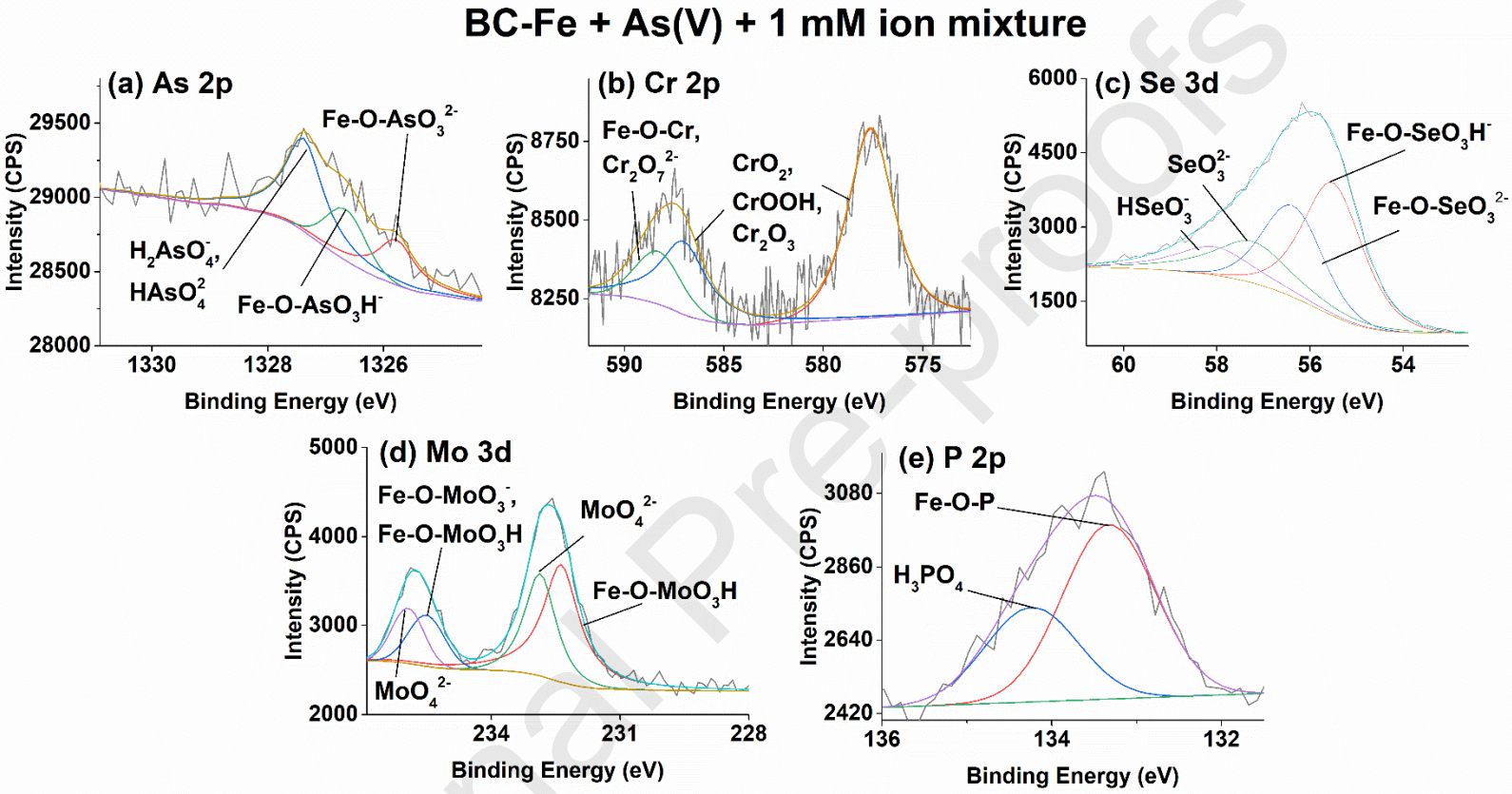

622

623 **Figure 4.** Deconvoluted high resolution (HR)-XPS BC-Fe laden with 10 mg/L As(V) plus
624 multi-ion mixtures at 1 mM (CPS-Counts for second) for (a) As 2 p, (b) Cr 2p, (c) Se 3d,
625 (d) Mo 3d, (e) P 2p.

626

627 The possible sorption interactions and pathways of the competitive contaminants
628 and arsenic on BC and BC-Fe surfaces are summarized in scheme 1. Interactions can occur
629 through electrostatic attractions, hydrogen bonding and weak chemisorption to BC

630 phenolics. On iron oxide surface chemisorption dominates for phosphate, molybdate,
631 selenate, sulfate and chromate. Electrostatic attractions and hydrogen bonding may play a
632 role in carbonate, nitrate, fluoride and chloride sorption. In addition, the stoichiometric
633 precipitation of metal (Mg, Ca and Fe)-oxyanion (phosphate, molybdate, selenate and
634 chromate) insoluble compounds has to be considered.

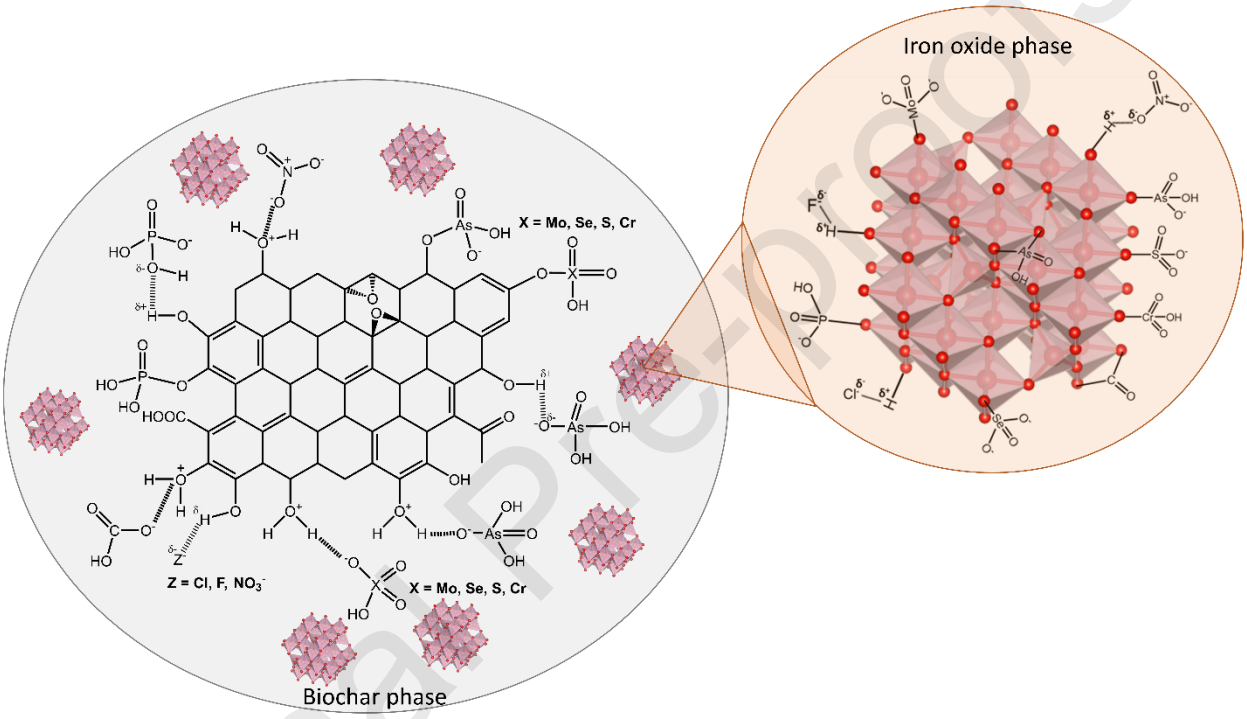

635

636 **Scheme 1.** Schematic representation of possible interactions of arsenate and competitive
637 contaminants ions on BC and iron oxide phases of BC-Fe

638 The As(V) chemisorption mechanism onto magnetite is summarized in scheme 2.
639 As(V) adsorbs on magnetite's 111 outer planes as monodentate links to a single iron or via
640 bidentate binding to a single iron atom or to two adjacent surface iron atoms. Associative or
641 dissociative pathways could exist. The crystal chemistry and DFT calculations presented by
642 Sherman and Randall [74] defined the possible surface arsenate structures and their
643 conjugate acids chemisorbed onto various iron oxides (goethite, ferrihydrite, hematite and

644 lepidocrocite) as bidentate corner-sharing complexes (^{2}C), edge-sharing (^{2}E) and
645 monodentate corner-sharing (^{1}V) complexes. EXAFS and XANES As(III) studies can be
646 similarly compared to As(V) adsorption of magnetite by the formation of bidentate
647 binuclear corner-sharing complexes (^{2}C) [28, 75, 76]. The possible chemisorbed arsenate
648 surface species versus solution pH are shown in Scheme X. The 3-D octahedral structure
649 shown is simplified as structure **1**. These chemisorbed species have been widely proposed
650 from several experimental and theoretical studies. Monodentate neutral **2**, monodentate
651 monoanion **3**, and dianion **4**, can exist along with bidentate neutral **5**, and bimetallic
652 bidentate anion **6** depending on solution pH. Also, bidentate monometallic complexes at
653 edges or corners are possible (**7-10**), but their stabilities have not been established.
654 Tridentate trinuclear corner-sharing (^{3}C) complexes (**11**) were favored for As(III) on
655 magnetite [76]. Tetrahedral vacancies might allow tridentate As(V) adsorption [77].

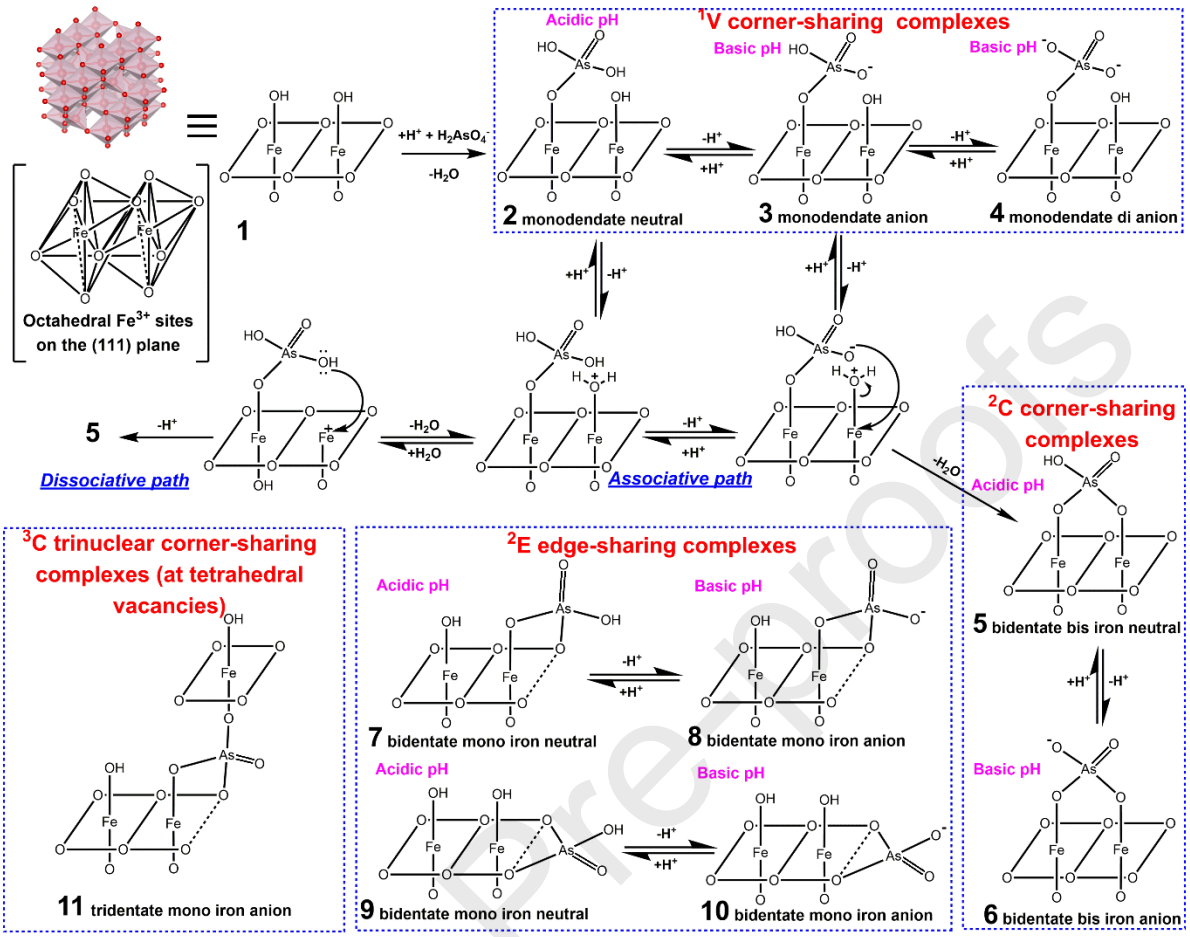

Scheme 2. Possible structures of arsenate-magnetite surface complexes.*These structures are based on the reported literature on FT-IR, XPS, Mossbauer, XANES and DFT studies for arsenate sorption on to various iron oxides (magnetite, maghemite, hematite, lepidocrocite, ferrihydrite and goethite). Possible hydrogen bonding between phosphate oxygen and hydroxyl with iron oxygens or hydroxyl groups to form pseudo-monodentate or resonance structures are not shown here.

3.5. Conclusions

An Fe_3O_4/*G. chacoensis* bamboo biochar composite (BC-Fe), which previously demonstrated remarkable As(V) Langmuir adsorption capacities (39-868 mg/g) and robust removal over a 5-9 pH window [37] is presented in multicomponent aqueous systems together with scale up applications for the first time in Latin America. Discarded, locally available, and silica-rich culms of *G. chacoensis* were transformed into a value-added engineered biochar adsorbent for arsenic removal from water. These chars are produced from single known species (native from Bolivia, Paraguay, Uruguay, Brazil, and Argentina) and thus, more readily duplicated than those produced from unknown culm fragments or unknown mixtures of a pool of known species.

The high correlation between the model predicted column capacity and the column capacity calculated by breakthrough curve integration indicates the breakthrough curve integration model explains the column adsorption data. Column capacities ranged 8.2-7.5 mg/g and were not affected by 5-9 pH shift. A faster flow rate was compensated by higher column height which increased the sorption site density. Capacities among this and our previous study were similar.

Attempting multicomponent studies is challenging due to multiple simultaneous interactions. Yet, such data is critical for modelling the adsorbents behavior in real water systems. The influence of other ions over arsenic uptake was higher for the raw-biochar (BC) than for BC-Fe. With the exception of nitrate, individually competing ions at low concentration (0.01 mM) did not significantly inhibit As(V) sorption onto BC-Fe. The presence of ten ions in low concentrations (0.01 mM) did not significantly influence BC-Fe´s preference for arsenate, and removal remained above 90 %. Fe_3O_4 enhanced arsenate

adsorption as well as phosphate, molybdate, dichromate and selenate. This enhances the idea that BC-Fe appears to provide safe As-drinking water in diverse aqueous medias. BC and BC-Fe´s deconvoluted XPS in multicomponent aqueous mixtures exhibit arsenate adsorption or potential arsenate adsorption sites affected by the presence of chromate, selenate, molybdate and phosphate. Adsorption pathways are proposed including electrostatic attractions, hydrogen bonding and chemisorption to BC phenolics.

The batch and column adsorption capacities of BC and BC-Fe and their ability to provide safe drinking water was evaluated using a naturally contaminated tap water (165 ± 5 µg/L As). BC-Fe in a 2 g/L dose (0.1 g of BC-Fe into 50 mL of solution) was sufficient to provide safe drinking water at 40 ^{o}C. A 960 mL volume of safe As drinking water (203.8 BV) was collected by using 1 g of BC-Fe. After this treatment, BC-Fe is considered a non-hazardous residue, BC-Fe can be disposed of inside a household bin.

Regeneration when the maximum adsorbent capacity is not completely As-saturated was challenging. Potassium phosphate was best for BC-Fe regeneration.

Fe_3O_4 nanoparticles dispersed on *G. chacoensis* bamboo biochar (BC-Fe) is capable to provide household-scale arsenic contaminated water treatment. Both batch and fixed-bed column remediations were investigated and proven to be effective in scaled-up technologies for large-scale implementations. A BC-Fe‘s *spinoff* technology for household As-free drinking water provision which considers practical functionality at low cost is presented. A better understanding of simple local sorption strategies for arsenic treatment on multicomponent aqueous systems will help bridge the gaps between environmental science and technology, and commercialization.

Acknowledgments

This work was supported by the University of Buenos Aires [grant UBACyT 20020160100061BA], the Mississippi State University Chemistry Department and Fulbright-Bunge & Born.

References

[1] B.K. Mandal, K.T. Suzuki, Arsenic round the world: a review, Talanta 58(1) (2002) 201-235.
[2] D.K. Nordstrom, Worldwide occurrences of arsenic in ground water, American Association for the Advancement of Science, 2002.
[3] A.E. Bardach, A. Ciapponi, N. Soto, M.R. Chaparro, M. Calderon, A. Briatore, N. Cadoppi, R. Tassara, M.I. Litter, Epidemiology of chronic disease related to arsenic in Argentina: A systematic review, Sci Total Environ 538 (2015) 802-16.
[4] M.I. Litter, M.E. Morgada, J. Bundschuh, Possible treatments for arsenic removal in Latin American waters for human consumption, Environ Pollut 158(5) (2010) 1105-18.
[5] S. Islam, M.M. Rahman, M. Islam, R. Naidu, Geographical variation and age-related dietary exposure to arsenic in rice from Bangladesh, Science of the Total Environment 601 (2017) 122-131.
[6] H. Rasheed, P. Kay, R. Slack, Y.Y. Gong, A. Carter, Human exposure assessment of different arsenic species in household water sources in a high risk arsenic area, Science of the Total Environment 584 (2017) 631-641.
[7] E. Astolfi, A. Maccagno, J.G. Fernández, R. Vaccaro, R. Stimola, Relation between arsenic in drinking water and skin cancer, Biological Trace Element Research 3(2) (1981) 133-143.
[8] W.-P. Tseng, Effects and dose-response relationships of skin cancer and blackfoot disease with arsenic, Environmental health perspectives 19 (1977) 109-119.
[9] T. Yoshida, H. Yamauchi, G. Fan Sun, Chronic health effects in people exposed to arsenic via the drinking water: dose-response relationships in review, Toxicol Appl Pharmacol 198(3) (2004) 243-52.
[10] W.H.O. WHO, Preventing disease through healthy environment. Exposure to arsenic: a major public health concern, Public Health and Environment, 20 Avenue Appia, 1211 Geneva 27, Switzerland, 2010.
[11] J. Bundschuh, M. Litter, V.S. Ciminelli, M.E. Morgada, L. Cornejo, S.G. Hoyos, J. Hoinkis, M.T. Alarcon-Herrera, M.A. Armienta, P. Bhattacharya, Emerging mitigation needs and sustainable options for solving the arsenic problems of rural and isolated urban areas in Latin America - a critical analysis, Water Res 44(19) (2010) 5828-45.
[12] R. Kumar, M. Patel, P. Singh, J. Bundschuh, C.U. Pittman, Jr., L. Trakal, D. Mohan, Emerging technologies for arsenic removal from drinking water in rural and peri-urban areas: Methods, experience from, and options for Latin America, Sci Total Environ 694 (2019) 133427.
[13] D. Mohan, C.U. Pittman, Jr., Arsenic removal from water/wastewater using adsorbents--A critical review, J Hazard Mater 142(1-2) (2007) 1-53.
[14] M.I. Litter, A.M. Ingallinella, V. Olmos, M. Savio, G. Difeo, L. Botto, E.M.F. Torres, S. Taylor, S. Frangie, J. Herkovits, I. Schalamuk, M.J. Gonzalez, E. Berardozzi, F.S. Garcia Einschlag, P. Bhattacharya, A. Ahmad, Arsenic in Argentina: Technologies for arsenic removal from groundwater sources, investment costs and waste management practices, Sci Total Environ 690 (2019) 778-789.
[15] M.I. Litter, A.M. Ingallinella, V. Olmos, M. Savio, G. Difeo, L. Botto, E.M. Farfan Torres, S. Taylor, S. Frangie, J. Herkovits, I. Schalamuk, M.J. Gonzalez, E. Berardozzi, F.S. Garcia Einschlag, P.

Bhattacharya, A. Ahmad, Arsenic in Argentina: Occurrence, human health, legislation and determination, Sci Total Environ 676 (2019) 756-766.
[16] J. Kim, J. Song, S.-M. Lee, J. Jung, Application of iron-modified biochar for arsenite removal and toxicity reduction, Journal of Industrial and Engineering Chemistry 80 (2019) 17-22.
[17] S. Alvarado, M. Guedez, M.P. Lue-Meru, G. Nelson, A. Alvaro, A.C. Jesus, Z. Gyula, Arsenic removal from waters by bioremediation with the aquatic plants Water Hyacinth (Eichhornia crassipes) and Lesser Duckweed (Lemna minor), Bioresour Technol 99(17) (2008) 8436-40.
[18] J.W. Huang, C.Y. Poynton, M.P. Elles, Phytofiltration of Arsenic from Drinking Water Using Arsenic-Hyperaccumulating Ferns, Environmental science & technology 38(12) (2004) 3412-3417.
[19] O. Gibert, J. De Pablo, J. Cortina, C. Ayora, Treatment of acid mine drainage by sulphate-reducing bacteria using permeable reactive barriers: a review from laboratory to full-scale experiments, Reviews in Environmental Science and Biotechnology 1(4) (2002) 327-333.
[20] A.G. Karunanayake, C. Navarathna, S. Gunatilake, M. Crowley, R. Anderson, D. Mohan, F. Perez, C.U. Pittman, T.E. Mlsna, Fe3O4 Nanoparticles Dispersed on Douglas Fir Biochar for Phosphate Sorption, ACS Applied Nano Materials (2019).
[21] S. Wang, B. Gao, A.R. Zimmerman, Y. Li, L. Ma, W.G. Harris, K.W. Migliaccio, Removal of arsenic by magnetic biochar prepared from pinewood and natural hematite, Bioresour Technol 175 (2015) 391-5.
[22] K.Z. Benis, A.M. Damuchali, J. Soltan, K. McPhedran, Treatment of aqueous arsenic–A review of biochar modification methods, Science of The Total Environment (2020) 139750.
[23] X. Tan, Y. Liu, G. Zeng, X. Wang, X. Hu, Y. Gu, Z. Yang, Application of biochar for the removal of pollutants from aqueous solutions, Chemosphere 125 (2015) 70-85.
[24] R. Deng, D. Huang, G. Zeng, J. Wan, W. Xue, X. Wen, X. Liu, S. Chen, J. Li, C. Liu, Decontamination of lead and tetracycline from aqueous solution by a promising carbonaceous nanocomposite: Interaction and mechanisms insight, Bioresource technology 283 (2019) 277-285.
[25] S. Rajput, C.U. Pittman Jr, D. Mohan, Magnetic magnetite (Fe3O4) nanoparticle synthesis and applications for lead (Pb2+) and chromium (Cr6+) removal from water, Journal of colloid and interface science 468 (2016) 334-346.
[26] C.M. Navarathna, N. Bombuwala Dewage, C. Keeton, J. Pennisson, R. Henderson, B. Lashley, X. Zhang, E.B. Hassan, F. Perez, D. Mohan, Biochar Adsorbents with Enhanced Hydrophobicity for Oil Spill Removal, ACS Applied Materials & Interfaces 12(8) (2020) 9248-9260.
[27] N.B. Dewage, A.S. Liyanage, Q. Smith, C.U. Pittman Jr, F. Perez, D. Mohan, T. Mlsna, Fast Aniline and Nitrobenzene Remediation from Water on Magnetized and Nonmagnetized Douglas Fir Biochar, Chemosphere 225 (2019) 943-953.
[28] P. Singh, A. Sarswat, C.U. Pittman Jr, T. Mlsna, D. Mohan, Sustainable Low-Concentration Arsenite [As (III)] Removal in Single and Multicomponent Systems Using Hybrid Iron Oxide–Biochar Nanocomposite Adsorbents—A Mechanistic Study, ACS omega 5(6) (2020) 2575-2593.
[29] X. Londoño, P.M. Peterson, Guadua chacoensis (Poaceae: Bambuseae), its taxonomic identity, morphology, and affinities., Novon 2 (1992) 41-46.
[30] M.A. Lizarazu, A.S. Vega, *Guadua*, in: F.O. Zuloaga, Z.E. Rúgolo, A.M. Anton (Eds.), Flora Argentina. Plantas Vasculares de la República Argentina. Monocotyledoneae: Poaceae: Aristidoideae-Pharoideae2012, pp. 59-63.
[31] M.A. Lizarazu, Z.E. Rúgolo de Agrasar, A.S. Vega, A New Species of <I>Guadua</I> (Poaceae, Bambusoideae, Bambuseae) and Synopsis of the Genus in Argentina and Neighboring Regions, Systematic Botany 38(4) (2013) 1062-1075.
[32] A.S. Vega, Z.E. Rúgolo, *Guadua* Kunth, in: Z.E. Rúgolo (Ed.), Bambúes leñosos nativos y exóticos de la argentina, Trama S.A, CABA, Argentina, 2016, pp. 99-112.

[33] M. Lindholm, S. Palm, *Guadua chacoensis* in Bolivian investigation of mechanical properties of a bamboo species, Department of Management and Engineering Centre for Wood Technology & Design, University of Linköping, Sweden, 2007.
[34] J.P. Haggar, C.B. Briscoe, R.P. Butterfield, Native species: a resource for the diversification of forestry production in the lowland humid tropics, Forest Ecology and Management 106 (1998) 195-203.
[35] C.C. Panizzo, P.V. Fernandez, D. Colombatto, M. Ciancia, A.S. Vega, Anatomy, nutritional value and cell wall chemical analysis of foliage leaves of Guadua chacoensis (Poaceae, Bambusoideae, Bambuseae), a promising source of forage, J Sci Food Agric 97(4) (2017) 1349-1358.
[36] P.V. Fernandez, V.M. Zelaya, L. Cobello, A.S. Vega, M. Ciancia, Glucuronoarabinoxylans and other cell wall polysaccharides from shoots of Guadua chacoensis obtained by extraction in different conditions, Carbohydr Polym 226 (2019) 115313.
[37] J. Alchouron, C. Navarathna, H.D. Chludil, N.B. Dewage, F. Perez, C.U. Pittman Jr, A.S. Vega, T.E. Mlsna, Assessing South American Guadua chacoensis bamboo biochar and Fe3O4 nanoparticle dispersed analogues for aqueous arsenic (V) remediation, Science of The Total Environment 706 (2020) 135943.
[38] M. Fu, Sustainable management and utilization of sympodial bamboos, China Forestry Publishing House2007.
[39] A.G. Karunanayake, O.A. Todd, M.L. Crowley, L.B. Ricchetti, C.U.J. Pittman, R. Anderson, T.E. Mlsna, Rapid removal of salicylic acid, 4-nitroaniline, benzoic acid and phthalic acid from wastewater using magnetized fast pyrolysis biochar from waste Douglas fir, Chemical Engineering Journal 319 (2017) 75-88.
[40] C.J. Geankoplis, Transport processes and separation process principles:(includes unit operations), Prentice Hall Professional Technical Reference2003.
[41] S. Ghorai, K.K. Pant, Equilibrium, kinetics and breakthrough studies for adsorption of fluoride on activated alumina, Separation and Purification Technology 42(3) (2005) 265-271.
[42] R. Singh, S. Singh, P. Parihar, V.P. Singh, S.M. Prasad, Arsenic contamination, consequences and remediation techniques: a review, Ecotoxicol Environ Saf 112 (2015) 247-70.
[43] S. Hasan, A. Krishnaiah, T.K. Ghosh, D.S. Viswanath, V.M. Boddu, E.D. Smith, Adsorption of divalent cadmium (Cd (II)) from aqueous solutions onto chitosan-coated perlite beads, Industrial & engineering chemistry research 45(14) (2006) 5066-5077.
[44] S.S.A. Alkurdi, I. Herath, J. Bundschuh, R.A. Al-Juboori, M. Vithanage, D. Mohan, Biochar versus bone char for a sustainable inorganic arsenic mitigation in water: What needs to be done in future research?, Environ Int 127 (2019) 52-69.
[45] T. Wen, J. Wang, S. Yu, Z. Chen, T. Hayat, X. Wang, Magnetic Porous Carbonaceous Material Produced from Tea Waste for Efficient Removal of As(V), Cr(VI), Humic Acid, and Dyes, ACS Sustainable Chemistry & Engineering 5(5) (2017) 4371-4380.
[46] A. Sigdel, J. Park, H. Kwak, P.-K. Park, Arsenic removal from aqueous solutions by adsorption onto hydrous iron oxide-impregnated alginate beads, Journal of Industrial and Engineering Chemistry 35 (2016) 277-286.
[47] Q. Yang, Y. Zhong, X. Li, X. Li, K. Luo, X. Wu, H. Chen, Y. Liu, G. Zeng, Adsorption-coupled reduction of bromate by Fe (II)–Al (III) layered double hydroxide in fixed-bed column: experimental and breakthrough curves analysis, Journal of Industrial and Engineering Chemistry 28 (2015) 54-59.
[48] H. Patel, Fixed-bed column adsorption study: a comprehensive review, Applied Water Science 9(3) (2019).

[49] Z. Ding, X. Xu, T. Phan, X. Hu, G. Nie, High adsorption performance for As(III) and As(V) onto novel aluminum-enriched biochar derived from abandoned Tetra Paks, Chemosphere 208 (2018) 800-807.
[50] X. Hu, Z. Ding, A.R. Zimmerman, S. Wang, B. Gao, Batch and column sorption of arsenic onto iron-impregnated biochar synthesized through hydrolysis, Water Res 68 (2015) 206-16.
[51] P. Roy, N.K. Mondal, S. Bhattacharya, B. Das, K. Das, Removal of arsenic(III) and arsenic(V) on chemically modified low-cost adsorbent: batch and column operations, Applied Water Science 3(1) (2013) 293-309.
[52] B. Te, B. Wichitsathian, C. Yossapol, W. Wonglertarak, Investigation of Arsenic Removal from Water by Iron-Mixed Mesoporous Pellet in a Continuous Fixed-Bed Column, Water, Air, & Soil Pollution 229(9) (2018).
[53] B. Te, B. Wichitsathian, C. Yossapol, W. Wonglertarak, Development of low-cost iron mixed porous pellet adsorbent by mixture design approach and its application for arsenate and arsenite adsorption from water, Adsorption Science & Technology 36(1-2) (2017) 372-392.
[54] Y. Wei, S. Wei, C. Liu, T. Chen, Y. Tang, J. Ma, K. Yin, S. Luo, Efficient removal of arsenic from groundwater using iron oxide nanoneedle array-decorated biochar fibers with high Fe utilization and fast adsorption kinetics, Water Res 167 (2019) 115107.
[55] J. Nikic, J. Agbaba, M.A. Watson, A. Tubic, M. Solic, S. Maletic, B. Dalmacija, Arsenic adsorption on Fe-Mn modified granular activated carbon (GAC-FeMn): batch and fixed-bed column studies, J Environ Sci Health A Tox Hazard Subst Environ Eng 54(3) (2019) 168-178.
[56] M. Kalaruban, P. Loganathan, T.V. Nguyen, T. Nur, M.A. Hasan Johir, T.H. Nguyen, M.V. Trinh, S. Vigneswaran, Iron-impregnated granular activated carbon for arsenic removal: Application to practical column filters, J Environ Manage 239 (2019) 235-243.
[57] R. Senthilkumar, D.M. Reddy Prasad, L. Govindarajan, K. Saravanakumar, B.S. Naveen Prasad, Synthesis of green marine algal-based biochar for remediation of arsenic(V) from contaminated waters in batch and column mode of operation, Int J Phytoremediation (2019) 1-8.
[58] J. Yan, Y. Xue, L. Long, Y. Zeng, X. Hu, Adsorptive removal of As(V) by crawfish shell biochar: batch and column tests, Environ Sci Pollut Res Int 25(34) (2018) 34674-34683.
[59] J.S. Lee, J.O. Nriagu, Stability constants for metal arsenates, Environmental Chemistry 4(2) (2007) 123-133.
[60] Y. Fang, A novel intracellular protein delivery system-Magnesium phosphate nanoparticles with cationic lipid coating for catalase intracellular delivery, (2014).
[61] D. Jiang, B. Chu, Y. Amano, M. Machida, Removal and recovery of phosphate from water by Mg-laden biochar: Batch and column studies, Colloids and Surfaces A: Physicochemical and Engineering Aspects 558 (2018) 429-437.
[62] C. Mansour, G. Lefèvre, E. Pavageau, H. Catalette, M. Fédoroff, S. Zanna, Sorption of sulfate ions onto magnetite, Journal of colloid and interface science 331(1) (2009) 77-82.
[63] B. Verbinnen, C. Block, D. Hannes, P. Lievens, M. Vaclavikova, K. Stefusova, G. Gallios, C. Vandecasteele, Removal of Molybdate Anions from Water by Adsorption on Zeolite-Supported Magnetite, Water environment research 84(9) (2012) 753-760.
[64] A.G. Karunanayake, C.M. Navarathna, S.R. Gunatilake, M. Crowley, R. Anderson, D. Mohan, F. Perez, C.U.J. Pittman, T. Mlsna, Fe3O4 Nanoparticles Dispersed on Douglas Fir Biochar for Phosphate Sorption, ACS Applied Nano Materials 2(6) (2019) 3467-3479.
[65] D. Mohan, A. Sarswat, Y.S. Ok, C.U. Pittman, Jr., Organic and inorganic contaminants removal from water with biochar, a renewable, low cost and sustainable adsorbent--a critical review, Bioresour Technol 160 (2014) 191-202.
[66] T.G. Asere, C.V. Stevens, G. Du Laing, Use of (modified) natural adsorbents for arsenic remediation: A review, Sci Total Environ 676 (2019) 706-720.

[67] C.-H. Liu, Y.-H. Chuang, T.-Y. Chen, Y. Tian, H. Li, M.-K. Wang, W. Zhang, Mechanism of arsenic adsorption on magnetite nanoparticles from water: thermodynamic and spectroscopic studies, Environmental science & technology 49(13) (2015) 7726-7734.
[68] R. Li, J.J. Wang, L.A. Gaston, B. Zhou, M. Li, R. Xiao, Q. Wang, Z. Zhang, H. Huang, W. Liang, An overview of carbothermal synthesis of metal–biochar composites for the removal of oxyanion contaminants from aqueous solution, Carbon 129 (2018) 674-687.
[69] N. Bombuwala Dewage, A.S. Liyanage, C.U. Pittman, Jr., D. Mohan, T. Mlsna, Fast nitrate and fluoride adsorption and magnetic separation from water on alpha-Fe2O3 and Fe3O4 dispersed on Douglas fir biochar, Bioresour Technol 263 (2018) 258-265.
[70] EPA, Toxicity characteristics leaching procedure, Method 1311., (1992).
[71] Decreto831/93, Residuos peligrosos. Generación, transporte y disposición de residuos peligrosos, in: R.d.l.l. 24.051. (Ed.) Ministerio de justicia y derechos humanos de la, Presidencia de la Nación Argentina, 1993.
[72] L. Verma, J. Singh, Synthesis of novel biochar from waste plant litter biomass for the removal of Arsenic (III and V) from aqueous solution: A mechanism characterization, kinetics and thermodynamics, J Environ Manage 248 (2019) 109235.
[73] T.S. Anirudhan, M.R. Unnithan, Arsenic(V) removal from aqueous solutions using an anion exchanger derived from coconut coir pith and its recovery, Chemosphere 66(1) (2007) 60-6.
[74] D.M. Sherman, S.R. Randall, Surface complexation of arsenic (V) to iron (III)(hydr) oxides: structural mechanism from ab initio molecular geometries and EXAFS spectroscopy, Geochimica et Cosmochimica Acta 67(22) (2003) 4223-4230.
[75] C.M. Navarathna, A.G. Karunanayake, S.R. Gunatilake, C.U. Pittman Jr, F. Perez, D. Mohan, T. Mlsna, Removal of Arsenic (III) from water using magnetite precipitated onto Douglas fir biochar, Journal of environmental management 250 (2019) 109429.
[76] J. Farrell, B.K. Chaudhary, Understanding arsenate reaction kinetics with ferric hydroxides, Environmental science & technology 47(15) (2013) 8342-8347.
[77] Y. Wang, G. Morin, G. Ona-Nguema, N. Menguy, F. Juillot, E. Aubry, F. Guyot, G. Calas, G.E. Brown Jr, Arsenite sorption at the magnetite–water interface during aqueous precipitation of magnetite: EXAFS evidence for a new arsenite surface complex, Geochimica et Cosmochimica Acta 72(11) (2008) 2573-2586.